Langmuir

Article

pubs.acs.org/Langmuir

Chemical Characterization of DNA-Immobilized InAs Surfaces Using X-ray Photoelectron Spectroscopy and Near-Edge X-ray Absorption Fine Structure

EunKyung Cho,[†] April Brown,[‡] and Thomas F. Kuech*,[†]

[†]Department of Chemical and Biological Engineering, University of Wisconsin—Madison, 1415 Engineering Drive, Madison, Wisconsin 53706, United States

[‡]Department of Electrical and Computer Engineering, Duke University, Durham, North Carolina 27708, United States

Supporting Information

ABSTRACT: Single-stranded DNA immobilized on an III−V semiconductor is a potential high-sensitivity biosensor. The chemical and electronic changes occurring upon the binding of DNA to the InAs surface are essential to understanding the DNA-immobilization mechanism. In this work, the chemical properties of DNA-immobilized InAs surfaces were determined through high-resolution X-ray photoelectron spectroscopy (XPS) and near-edge X-ray absorption fine structure (NEXAFS). Prior to DNA functionalization, HF- and NH_4OH- based aqueous etches were used to remove the native oxide from the InAs surface. The initial chemical state of the surface resulting from these etches were characterized prior to functionalization. F-tagged thiolated single-stranded DNA (ssDNA) was used as the probe species under two different functionalization methods. The presence of DNA immobilized on the surface was confirmed from the F 1s, N 1s, and P 2p peaks in the XPS spectra. The presence of salt had a profound effect on the density of immobilized DNA on the InAs surface. To study the interfacial chemistry, the surface was treated with thiolated ssDNA with and without the mercaptohexanol molecule. An analysis of the As 3d and In 3d spectra indicates that both In−S and As−S are present on the surface after DNA functionalization. The amount of In−S and As−S was determined by the functionalization method as well as the presence of mercaptohexanol during functionalization. The orientation of the adsorbed ssDNA is determined by polarization-dependent NEXAFS utilizing the N K-edge. The immobilized ssDNA molecule has a preferred tilt angle with respect to the substrate normal, but with a random azimuthal distribution.

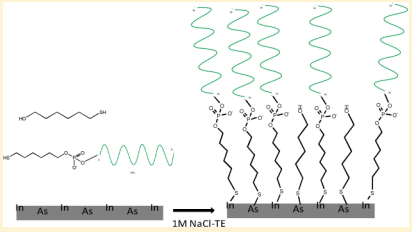

INTRODUCTION

DNA immobilization on solid surfaces is the basis of many biotechnical applications, such as DNA microarrays[1,2] and biosensors.[1,3] Previous research on DNA-modified surfaces has largely explored functionalized gold[4−7] and oxidized silicon or glass surfaces.[8−10] The desire to integrate biosensors, based on surface DNA, with preexisting electronic devices and circuits[11] requires the immobilization of DNA on various semiconducting materials.[12] III−V semiconductors, such as GaAs and InAs, can provide advantages in such applications over Si because of their differing surface chemistry, band structure, and electronic properties.[13] Recent studies have shown that such III−V semiconductors can be effectively used in chemical and biological sensing appplications.[14−16] Among III−V materials, indium arsenide (InAs) has a number of potential advantages as a substrate for DNA immobilization. InAs possesses a Fermi level at the surface typically positioned above the conduction band edge. This Fermi-level position leads to the presence of a 2D electron gas (2DEG) or electron accumulation layer on the surface. This electron accumulation layer can be modulated by surface treatments, allowing InAs to serve as a useful and sensitive sensing platform.[17,18] A variety of specific experimental stimuli can lead to changes in the surface band bending that alters electron accumulation or depletion, including surface defects,[19,20] surface adsorption of gas molecules,[21] or surface treatments with inorganic[14,22,23] and organic molecules.[24,25] This sensitivity suggests that InAs could be an excellent sensing platform.

The use of InAs in an electronic device or chemical and biological sensing application requires control of the InAs surface properties. The surface chemical passivation of InAs, using inorganic and organic materials, has resulted in well-defined chemical and electronic properties that are required for sensing applications.[26−28] For example, the surface structure and electronic states of InAs treated with ammonium sulfide solutions ($(NH_4)_2S_x$) have been investigated.[14,29] Sulfide-based passivation removes native oxides and other contaminants, leaving a covalently bonded sulfur layer possessing good short-term stability in ambient air and aqueous solutions compared to that of nonpassivized InAs. Other sulfur-based chemical preparations have used a weakly basic solution of thioacetamide as an alternative to inorganic sulfide passivation.[26] A study of

Received: June 7, 2012
Revised: July 17, 2012
Published: July 18, 2012

self-assembled monolayers (SAMs) of methyl-terminated alkanethiols has shown that these molecules are bonded to InAs through the thiol end-groups, which were found to be effective in chemically and electronically passivating the surfaces in an aqueous buffer such as phosphate-buffered saline (PBS) buffer (pH 7.4) but not in deionized water.[24] The chemical bonding of amino acids onto InAs surfaces has also been studied, and the amino acids were shown to block subsequent oxide growth on the InAs surface depending on the type of oxides present on the surfaces as well as the amine functional groups.[30,31] Although aspects of InAs surface passivation and functionalization have been investigated, functionalization with single-stranded DNA (ssDNA) has been left unexamined on InAs surfaces despite its potential utility as an electronic biosensor.

In this study, we have investigated the immobilization of thiolated ssDNA probes on n-type InAs(100) surfaces. The immobilized ssDNA/InAs serves as the basis of a nucleic acid affinity-based sensing platform. Aqueous-based chemical etches using a weakly basic solution or diluted hydrogen fluoride were used to remove the InAs surface oxide. The ssDNA probe was subsequently immobilized on the InAs surface using two different functionalization approaches. Thiolated ssDNA, with and without the coaddition of mercaptohexanol, was investigated to distinguish between differing chemistries associated with ssDNA immobilization on the InAs surface. X-ray photoelectron spectroscopy (XPS) and near-edge X-ray absorption fine structure spectroscopy (NEXAFS) were used to characterize the interfacial chemistry between the DNA probe and the InAs substrate and the polarization dependence of the ssDNA immobilized on the InAs substrate.

EXPERIMENTAL DETAILS

Materials. InAs(100) n-type, S-doped samples were cut from a single-side-polished wafer (WaferTech). The InAs samples were sequentially degreased in trichloroethylene (TCE), acetone, and methanol for 3 min each. The samples were initially etched by soaking in either an HF- or an NH_4OH-based solution. The HF solution consisted of as-received HF (49% HF, Honeywell) diluted in methanol to 5% volume concentration. The NH_4OH solution was prepared by a 1:1 volume mixture of the 29.7% NH_4OH stock solution (Fisher Scientific) and deionized water. The InAs samples were rinsed with deionized water and dried with flowing nitrogen before being transferred to an ultrahigh vacuum (UHV) chamber.

The ssDNA probes (Integrated DNA Technologies, Inc.) contained 25-base oligonucleotides with the following sequence: 5′-$HO(CH_2)_6$–S–S–$(CH_2)_6$–CCTCTGACTTCAACAGCGACACCCA–F-3′. The 5′ end of the probes was modified with a C6 thiol as an anchor to the InAs surface, and the 3′ end of the probe was modified with fluoroadenosine to verify the existence of DNA on the surface. The as-received thiolated probes were treated with tris(2-carboxyethyl)-phosphine (TCEP) solution that served to cleave the S–S bond at the 5′-end modifier. In this case, the thiolated ssDNA probe (HS-ssDNA) as well as $HO–(CH_2)_6–SH$ (mercaptohexanol, MCH) existed in the functionalization solution. HS-ssDNA without the MCH was also prepared using a different 5′ thiol modifier, $TS–(CH_2)_6–$, where T is a trityl group. The trityl group was removed by oxidation with silver nitrate, with the excess silver nitrate being precipitated with dithiothreitol (DTT). The excess DTT was removed by desalting in a NAP-25 column (GE Healthcare).

Sample Preparation. Samples labeled Cxy in this paper are used to designate the surface preparation, x, and functionalization procedure, y. Samples were prepared via an etching and annealing process. All of the prepared samples are summarized in Table 1. The as-received InAs that was rinsed with TCE, acetone, and methanol before the etching procedure is referred to as C0, C1, and C2 samples

Table 1. Sample Nomenclature

	cleaning method	functionalization solution
C0		
C1	NH_4OH etch	
C2	HF etch	
C3	HF etch and anneal at 380 °C	
C1A	NH_4OH etch	HS-ssDNA/MCH in a 1:9 mixture of NH_4OH in TE
C2A	HF etch	
C3A	HF etch and anneal at 380 °C	
C1B	NH_4OH etch	HS-ssDNA/MCH in TE
C2B	HF etch	
C3B	HF etch and anneal at 380 °C	
C1A–NaCl	NH_4OH etch	HS-ssDNA/MCH in a 1:9 mixture of NH_4OH in 1 M NaCl-TE
C1B–NaCl	NH_4OH etch	HS-ssDNA/MCH in 1 M NaCl-TE
C1A – no MCH	NH_4OH etch	HS-ssDNA in a 1:9 mixture of NH_4OH in 1 M NaCl-TE
C1B – no MCH	NH_4OH etch	HS-ssDNA in 1 M NaCl-TE

were NH_4OH etched for 10 min or HF etched for 3 min, respectively. Both etching procedures left ∼2.5 nm of residual oxide on the surface as measured with ellipsometry. C3 samples were HF etched for 3 min and annealed at 380 °C for 10 min in a UHV system. As a result of the annealing process, an InAs(100)-(4 × 2) reconstruction was observed using reflection high-energy electron diffraction (RHEED). The C0-, C1-, C2-, and C3-designated samples received no additional DNA treatment. To prepare DNA-immobilized InAs, the etched InAs samples were immersed in the functionalization solution. The functionalization solution for CxA samples was prepared with a 2 μM DNA + 200 μM TCEP solution in a 1:9 mixture of NH_4OH (29% stock solution) in tris-ethylenediaminetetraacetic acid (EDTA) (TE) buffer (Fluka, pH 7.4). The CxA samples were exposed to this solution for 1 h, with the temperature of the DNA-based solution held at 55 °C. The CxB samples were functionalized with a solution consisting of 2 μM DNA and 200 μM TCEP, diluted in TE buffer for 17 h at room temperature. The CxA–NaCl and CxB–NaCl samples were treated in a similar manner as the CxA and CxB samples, respectively, except that the functionalization solution consisted of 1 M NaCl–TE buffer instead of TE buffer. The CxA – no MCH and CxB – no MCH samples were prepared with ssDNA solution without MCH in 1 M NaCl–TE buffer. Each sample was rinsed with deionized water and dried under flowing nitrogen before analysis. The prepared samples were transported and stored in a VWR Desi-VacTM container with an automatic vacuum pump before insertion into the XPS analysis chamber. The container provides a clean, dry environment, but some reoxidation of the sample is expected because the vacuum in the container is ∼380 Torr, which is not sufficient to keep the surface completely oxide-free. The samples were inserted into the XPS chamber within 10 min with the exception of C3. The C3 sample had been stored for an hour in the container before being inserted into the UHV chamber.

XPS Characterization. The surfaces were characterized using X-ray photoelectron spectroscopy (XPS) with an Al Kα monochromatic source and a hemispherical electron energy analyzer. XPS measurements were carried out at room temperature in a UHV system with a base pressure of $<1 \times 10^{-9}$ Torr. The background chamber was monitored using a residual gas analyzer (Inficon Transpector) and was found to be composed of mostly hydrogen with small traces of nitrogen (<5%) and water (<2%). The high-resolution XPS scans were acquired using a 30° takeoff angle for the In 3d, As 3d, As 2p, C 1s, O 1s, N 1s, F 1s, P 2p, and S 2p spectral regions with 20 eV pass energy. Charge correction was performed using the adventitious C 1s peak at 285.0 eV. The peaks in the core-level spectra were fit using the Casa XPS software, version 2.3.15.[32] A convolution of Lorentzian and

dx.doi.org/10.1021/la302313v | Langmuir 2012, 28, 11890–11898

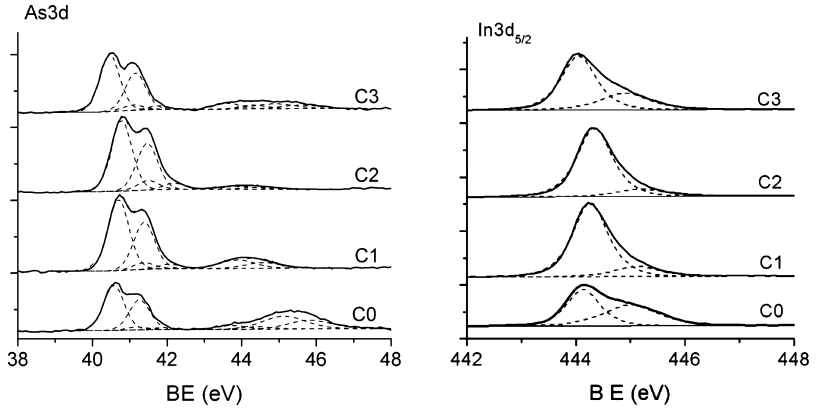

Figure 1. As 3d and In $3d_{5/2}$ spectrum of as-received and cleaned InAs samples: as-received InAs sample (C0); NH_4OH-etched InAs (C1); HF-etched InAs (C2); and HF-etched and annealed InAs (C3). The annealing step was carried out in UHV at 380 °C. A doublet separation of 0.69 eV for the As 3d region and 7.55 eV for the In 3d region was used, and the spin−orbit splitting intensity ratio was 0.67 for both spectra.

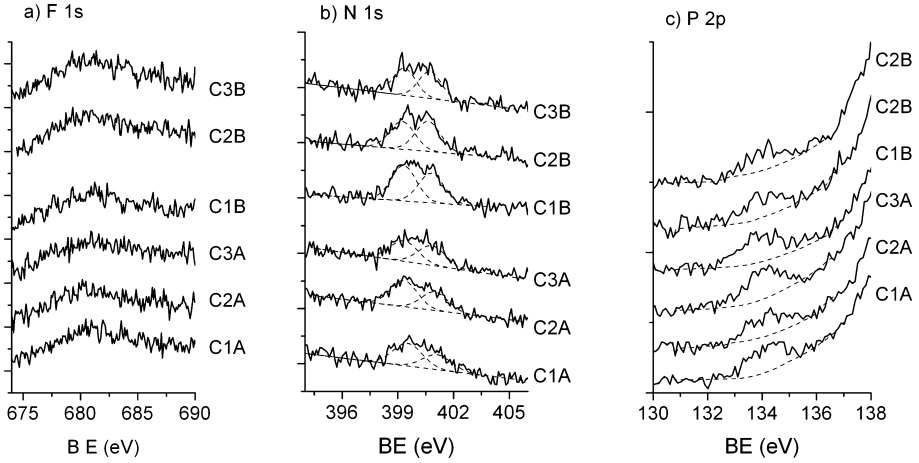

Figure 2. High-resolution XPS spectra of the (a) F 1s, (b) N 1s and (c) P 2p core levels from the functionalized samples (C1A, C2A, C3A, C1B, C2B, and C3B). Peak binding energies for the spectra were referenced to the adventitious C 1s component at 285.0 eV.

Gaussian line shapes was used to fit the peaks. Shirley and linear functions were used to model the signal background.[24,26,27]

NEXAFS Characterization. Near-edge X-ray absorption fine structure (NEXAFS) spectra were taken at the Synchrotron Radiation Center in Madison, Wisconsin using the HERMON beamline with total electron yield detection. The base pressure of the measurement chamber was $<2 \times 10^{-10}$ Torr. The X-rays were >90% linearly polarized. For each sample, scans were taken in the carbon K-edge region and nitrogen K-edge region at varying angles of the polarization vector with respect to the sample normal, between 90° (normal incidence) and 20° (grazing incidence). All NEXAFS spectra were normalized by the signal from a gold-coated 90% transmission grid placed in the path of the X-rays to eliminate the effect of incident beam intensity fluctuations. To account for the angle-dependent spot size, the spectra were normalized by the intensity in the preedge and postedge of the spectra.

RESULTS AND DISCUSSION

XPS Analysis of Clean InAs Surfaces. Prior to functionalization, the native oxide was removed. The C0, C1, C2, and C3 samples were prepared as summarized in Table 1 and were characterized as a reference for the DNA-functionalized InAs surfaces. Figure 1 presents the As 3d and In 3d spectra of the as-received and differentially cleaned surfaces. The As 3d spectrum of the as-received sample (C0) was resolved into the As−In (40.6 eV), elemental arsenic (41.2 eV), As_2O_3 (43.7 eV), and As_2O_5 (45.1 eV) peaks. The In 3d spectrum of sample C0 contains contributions from the In−As (444.1 eV) and In−O_x (445.0 eV) peaks. The separation of binding energies (BE) between the In−As and In−oxide components is found to be ~0.85 eV for sample C0. In fitting the spectra of C1, C2 and C3, the same BE separation was used to deconvolve the spectral features. As shown in Figure 1, the area under the oxide components in the As 3d and In 3d XPS spectra was significantly lower for both etched samples (C1 and C2) when compared to the native InAs sample (C0), indicating that there was substantial removal of the outer oxide layer. The HF etching (C2) was found to be the most effective in oxide removal. The as-received sample, C0, possessed two forms of arsenic oxide: As_2O_3 and As_2O_5. The As_2O_5 peak was not observed after either etching procedure (C1 and C2), but a small amount of As_2O_3 remained on the surface. Because the samples were exposed to air (less than 5 min) between etching and XPS analysis, some reoxidation of the etched samples could be expected. After annealing, the As_2O_5 peak at ~45 eV reappeared, in addition to the previously found As_2O_3 component in the As 3d spectrum of C3, with overall increases in the residual oxides noted in the In 3d and As 3d spectra. Although the annealing procedure was carried out at 380 °C under UHV conditions and an InAs(100)-(4 × 2) reconstruction was observed, the annealing temperature was not high enough to desorb all of the residual arsenic oxide on the

dx.doi.org/10.1021/la302313v | Langmuir 2012, 28, 11890−11898

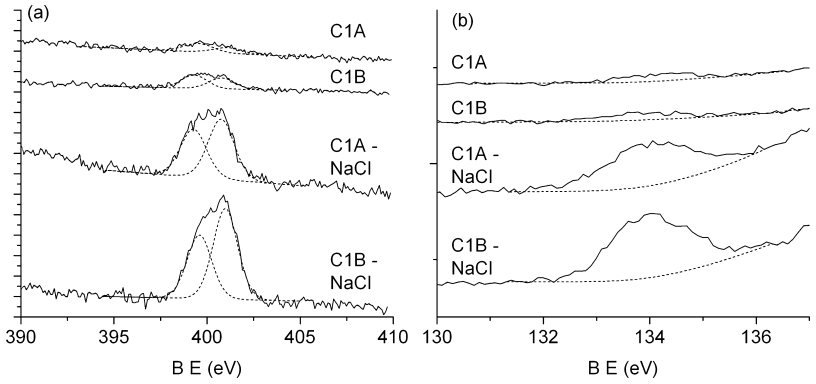

Figure 3. High-resolution XPS spectra of the (a) N 1s and (b) P 2p regions for the functionalized InAs obtained from C1A and C1B prepared with and without salt.

surface.[33] Considering that the reaction $As_2O_5 \rightarrow As_2O_3 + O_2$ occurs below 300 °C,[34] As_2O_5 should not have been found after the annealing procedure. However, an increase in the amounts of As_2O_5 and indium oxide was observed in the XPS spectra of the C3 sample and may be attributed to the longer air exposure of the sample as compared to that of the C1 and C2 samples. A thicker initial oxide is therefore not completely removed. In addition, higher annealing temperatures, while desorbing the oxide, lead to preferential As loss and a resulting In-rich surface. The In-to-As ratio calculated on the basis of the area of the In 3d and As 3d spectra was found to be 1.2 for C1 and C2 and 1.3 for C3. The As loss was therefore not considered to be significant at the employed annealing temperature of 380 °C.

Immobilized DNA on InAs. The chemically prepared substrates (C1−C3) were soaked in the DNA solution to immobilize the DNA probes on the InAs surface. Samples of C1A, C2A, C3A, C1B, C2B, and C3B differed by the functionalization method. InAs substrate elements (In 3d and As 3d) and ssDNA probe components (F 1s, N 1s, and P 2p) were examined using high-resolution XPS. Figure 2 presents the F 1s, N 1s, and P 2p core-level spectra of the functionalized InAs. The fluorine peak is not attenuated by the deposited molecules on the surface because fluorine exists on the 3′ end of the DNA probe, indicating that ssDNA was immobilized and attachment was through the thiol. The fluorine peak was also used to monitor possible radiation damage to the DNA probe during XPS examination. Breakage of the N-glycosidic bond and/or the DNA backbone would lead to a decrease in the F 1s peak area with X-ray exposure. No decrease in the F 1s peak area was noted after continuous exposure to X-rays for ∼10 h. DNA immobilization on the surfaces can also be confirmed by the presence of nitrogen from the nucleobases and phosphorus from the phosphate backbone. The N 1s spectrum was resolved into two peak components with BEs of ∼399.3 eV and ∼400.8 eV. The BE of the N 1s peaks is consistent with published results[35] found for immobilized ssDNA with a mixture of 4 bases (A, T, C, G) on gold. The N 1s component with a higher BE is attributed to bases containing an NH_2 group, and the lower BE peak is due to the imino species, which include N═C bonds.[36] The P 2p core level was observed at a BE of ∼134.0 eV. Because the P 2p region is adjacent to the As 3p region of InAs, we used a Tougaard background estimation for the P 2p peak. The experimental P-to-N atomic ratios, calculated from the XPS peak areas of N 1s and P 2p, were found to be 0.3−0.4. The stoichiometric ratio of P/N based on the DNA probe molecule is 0.3 and is similar to the experimentally derived values. The higher experimental ratio of P/N could be due to an overestimation of the area of the P 2p spectrum. It is interesting that the amount of DNA immobilized on the surface was not affected by the cleaning method prior to functionalization.

The addition of salt to the buffer solution during DNA immobilization on gold has been studied and has led to increased DNA attachment.[4,37] When functionalization occurs, the local electrostatic environment created at the InAs surface should be different from that observed for a gold surface. However, if we consider the repulsive electrostatic interaction due to charge along the backbone of ssDNA, then we may expect the immobilization of DNA on InAs to be similarly affected by salt addition. Because the cleaning method did not affect the amount of DNA immobilized on the InAs surface, the C1 cleaning procedure was used to minimize the total number of chemicals involved in this investigation of the effect of salt addition. XPS data obtained from samples immersed in 2.0 μM DNA solutions, prepared in 1.0 M NaCl−TE, are shown in Figure 3. The XPS N 1s peak areas of C1A and C1B samples prepared from 1 M NaCl−TE buffer grow 4−6-fold compared to those for C1A and C1B prepared without salt are shown in Figure 3, indicating that the salt in the solution enhances the DNA immobilization on InAs. The influence of the ionic strength of the salt solution in determining the surface coverage of DNA is expected, given that ssDNA is a negatively charged molecule with 25 ionizable phosphate groups. The intermolecular electrostatic repulsion between neighboring strands of DNA should be minimized under the high ionic strength conditions. The charged DNA strands are electrostatically shielded in the salt solution, thus allowing higher surface coverages of ssDNA.[4,37]

In addition to the observed changes in the N 1s spectra, significant differences in the C 1s spectra were also observed. Table 2 compares the high-resolution C 1s spectra for the functionalized samples with and without salt addition to the functionalization solution. The C 1s spectra were resolved into four peaks as summarized in Table 2: C−C and C−H (285 eV), C−N and C−O (287 eV), N−C(═O)−C, N−C(═N)−N, N═C−N, and N−C−O (288 eV), and N−C(═O)−N (289 eV).[35,38] The relative concentrations of the different carbon species indicate that with increasing DNA-related carbon peaks at∼287, ∼288, and ∼289 eV there is a corresponding decrease in the percentage of C−C and C−H species. The increased DNA density on the surface leads to an attenuation of the signal from DNA segments near the InAs

dx.doi.org/10.1021/la302313v | *Langmuir* 2012, 28, 11890−11898

Table 2. XPS High-Resolution C 1s Chemical Species of the Functionalized Samples

	percentage			
C 1s components (BE, eV)	C−C, C−H (285.0)	C−N, C−O (286.5−286.8)	N−C(=O)−C, N−C(=N)−N, N=C−N, N−C−O (288.0−288.4)	N−C(=O)−N (289.4−289.9)
C1A	77.34	14.68	4.57	3.41
C1B	73.48	16.16	7.13	3.23
C1A−NaCl	66.77	20.81	8.42	4.01
C1B−NaCl	62.36	22.84	10.04	4.76

surface. This result again supports a prior conclusion obtained from the N 1s and P 2p core-level spectra that the C1A−NaCl and C1B−NaCl samples have a higher density of DNA probes immobilized on the InAs surface.

Interface Chemistry. The ideal truncated InAs(100) surface is terminated with either an In plane or As plane possessing unsaturated or dangling bonds. Ideally, without reconstruction, the dangling bonds of In would be empty whereas those of the more electronegative As would contain two electrons each. A variety of surface reconstructions will occur, however, depending on the surface stoichiometry and temperature.[39] Many such reconstructions provide both In and As binding sites to adsorbed molecules. Thiolate adsorption via the formation of a single covalent bond to the surface brings a single electron to the surface, altering the existing electronic balance. This adsorption event can result in new surface states corresponding to the interaction of the thiolate and the surface atoms. The exact nature of the S−substrate bonds formed by thiolates to III−V semiconductor surfaces has been of continuing interest in the literature.[40,41]

XPS spectra of the As 3d, As $2p_{3/2}$, and In 3d peaks from the DNA-functionalized InAs surfaces are shown in Figure 4. Spectra in both in the As $2p_{3/2}$ (~1322 eV) and As 3d (~41 eV) regions were acquired. The sampling depth for As 2p at a 30° takeoff angle is ~1 nm.[42] The As peak components are assigned to As−In, As−S, and arsenic oxides. The In 3d spectrum consists of peaks associated with In−As, In−S, and/or In−O_x bonds. The binding energies of substrate components are summarized in Table 3 and are in agreement with those reported elsewhere.[24,27,43] The reported BE difference between the In−S and In−O_x peaks is ~0.35 eV[27,44] at the limit of resolution of the XPS measurements in this study, thus leading to difficulties in the resolution of the individual peaks with the present instrument. A fixed BE separation of 0.5 eV between the In−S and In−As components was therefore used to deconvolve the In 3d spectrum of the functionalized samples.[27] A comparison of the spectra to the In 3d spectra obtained from the C1 surface demonstrates that the In_2O_3 component was reduced through interaction with the functionalization solution, leaving the In−S component on the surface. A comparison of the As 3d core-level spectrum of the functionalized sample with that of the C1 sample (Figure 4a) indicates that a significant peak appears as a shoulder on the high-BE side of the As 3d peak after functionalization. This shoulder is attributed to an As−S derived peak. The observed BE difference between the As−In and As−S components is 0.9 ± 0.1 eV, consistent with other reports.[27,41] Given the reported 0.5 eV BE separation between As−In and the elemental As component,[24] this As−S component has an additional 0.4 eV higher BE than the elemental As component. This is more clearly seen by examining the As $2p_{3/2}$ region. As shown in Figure 4b, the As−S component is clearly observed at 1323.5 eV in the As $2p_{3/2}$ region. Therefore, the As 3d and As $2p_{3/2}$ spectra demonstrate that As−S bonds are formed during functionalization.

Preferential In−S bond formation, with a small fraction of As−S bonds, was observed for the C1B−NaCl sample. The C1B−NaCl surface chemistry is consistent with most of the previous InAs(100) studies that have shown that the thiolate species bond predominantly to In atoms, with only a small number of As−S bonds present.[14,24,26,27,45] This preferred In−S bonding has also been observed on InP(100) surfaces.[39,40] The C1A−NaCl sample was prepared using a NH_4OH-based DNA

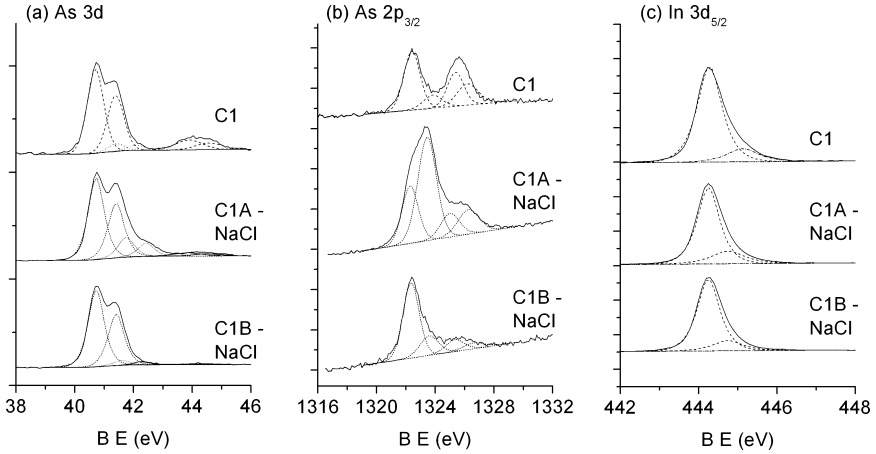

Figure 4. High-resolution XPS spectra of the (a) As 3d, (b) As $2p_{3/2}$, and (c) In $3d_{5/2}$ regions for clean, functionalized InAs.

Table 3. Binding Energy of the Main Components for As 3d, As $2p_{3/2}$, and In $3d_{5/2}$ Core Levels

	binding energy (eV)						
	In−As	As^0	As−S	As_2O_3	As_2O_5	In−S	In_2O_3
As $2p_{3/2}$	1322.3 ± 0.1	1324.0 ± 0.1	1323.5 ± 0.1	1325.3 ± 0.2	1326.6 ± 0.2		
As 3d	40.7 ± 0.1	41.2 ± 0.1	41.6 ± 0.1	44.0 ± 0.1	45.3 ± 0.1		
In $3d_{5/2}$	444.2 ± 0.1					444.7 ± 0.1	445.0 ± 0.1

solution possessed nearly equivalent In−S and As−S bonding formations (Table 4). Similar interfacial chemistry has been reported in cysteamine attachment on InAs.[42] Cysteamine was immobilized on the substrates via In−S and As−S bonds using ethanol-based solutions. The authors rationalized their results in terms of a model wherein the functionalization of InAs is kinetically limited and the predominance of In−S and As−S bonds depends on the relative rates of formation of those bonds. From these observations, it is clear that the binding depends significantly on the solution chemistry through direct reaction with the InAs surface, through the III−V elements present and/or their oxides. Previous work has shown that the NH_4OH solution removes the native oxide from the InAs sample during functionalization.[24,27] The As 3d and In 3d XPS spectra of CxA and CxB samples were also acquired. These data indicate that the surface preferentially possesses As−S bonds on CxA samples. In contrast, In−S bonds were dominant on CxB samples. The interfacial chemistry significantly depends on the functionalization method (A and B) rather than prior cleaning methods (C1, C2, and C3). Therefore, the surface chemistry or bond formation is primarily determined by the functionalization environment, not the cleaning methods prior to DNA immobilization.

Even though the In 3d and As 3d core-level peaks contain both In−S and As−S components on the functionalized surfaces, it is unclear whether this S−substrate bond originates uniquely from the DNA probe alone. The 5′ end of the DNA probe was modified with $HO(CH_2)_6$−S−S−$(CH_2)_6$−, and the S−S bond was cleaved by TCEP into $HO(CH_2)_6$−SH (hereafter mercaptohexanol, MCH) and HS−$(CH_2)_6$−ssDNA (hereafter HS−ssDNA). The mercaptohexanol was not removed from the functionalization solution and was present along with the HS−ssDNA. NEXAFS was used to verify which molecule was immobilized on the surface (Figure S1, Supporting Information). The C K-edge spectra consist of a series of features originating from HS−ssDNA and MCH. The peak at 287.3 eV was assigned to σ^*_{CH};[35] the peak at 288.5 eV was attributed to σ^*_{CO}.[46,47] The σ^*_{CNH} peak was found at 289 eV[35,48] and is characteristic of ssDNA alone. The C1A and C1B samples possessed σ^*_{CH} and σ^*_{CO} with no σ^*_{CNH} transition, which indicates that MCH is the dominant species immobilized on the surface. In the case of both C1A−NaCl and C1B−NaCl, σ^*_{CH}, σ^*_{CO}, and σ^*_{CNH} were observed. The σ^*_{CNH} peak intensity was also enhanced for the C1B−NaCl sample in comparison to that for the C1A−NaCl sample. These data indicate that both MCH and HS−ssDNA compete for the In and As bonds during functionalization, resulting in interfacial chemistry that depends on the reaction conditions (i.e., pH and temperature), with As−S and In−S bonds being preferred on the C1A−NaCl and C1B−NaCl surfaces, respectively.

Table 4. XPS Compositional Data for Functionalized Samples

sample	As−S/In−As	In−S/In−As	As/In
C1A−NaCl	0.25	0.25	1.09
C1B−NaCl	0.07	0.19	0.93
C1A − no MCH	0.06	0.16	0.88
C1B − no MCH	0.05	0.14	0.85

HS−ssDNA solution without MCH prepared in 1.0 M NaCl−TE was used to prepare the C1y − no MCH samples. The ratios of In−S to In−As and As−S to In−As and the surface stoichiometry, represented by the ratio of As to In, were calculated for C1y−NaCl and C1y − no MCH samples on the basis of the As 3d and In 3d XPS spectra as summarized in Table 4. Interestingly, preferred In−S bonding with a small fraction of As−S bonding was observed for the C1y − no MCH samples regardless of the functionalization methods. The immobilization efficiency of the HS−ssDNA probe on the InAs substrate is therefore not affected by changing the pH from 7.4 (TE solution) to 10.7 (TE/NH_4OH = 9:1). This is not surprising because the pK_a of the phosphodiester linkage in oligonucleotides is around 1[49] and the phosphodiester bond is extremely stable over this pH range.[50]

dx.doi.org/10.1021/la302313v | Langmuir 2012, 28, 11890−11898

The comparison of the surface chemistry of the samples with and without MCH indicates that because As−S bonding was found only for the C1A−NaCl sample, this As−S bonding originated from the MCH molecule and not from the HS−ssDNA probe. The mercaptohexanol present in the basic functionalization solution therefore preferentially binds to the As atoms on the surface. Thiol is a very weak acid with a pK_a of 8−10, and the pK_a of alkanethiol has a strong dependence on the alkanethiol chain length.[51] The thiol group in mercaptohexanol may be deprotonated in the NH_4OH-based functionalization solution (pH 10.7) because the pK_a of hexanethiol is 9.43.[52] Also, considering the substantially higher bond strength of the As−S bond (114 kcal/mol) in comparison to that of the In−S bond (69 ± 4 kcal/mol),[42] preferred As−S bonding on the surface is predicted. It is worth noting that alkanethiol SAMs on GaAs also exhibit preferential As−S bonding when using an NH_4OH-based solution.[41] C1B with and without MCH samples exhibits similar interfacial chemistry, showing that the MCH present in the C1B solution, which was not NH_4OH-based, was not effectively immobilized on the surface.

Optimal Functionalization Method. An optimal DNA immobilization procedure leading to the highest measured level of immobilized ssDNA was determined from the XPS elemental compositions from C1y samples prepared in ssDNA with and without MCH in a 1 M NaCl solution, as shown in Table 5. The optimal preparation method was based on the amount of adsorbed DNA on the InAs substrate. The nitrogen composition from the N 1s core-level spectrum for the functionalized samples is maximized on the C1B−NaCl surface. Interestingly, the C1y − no MCH samples result in less nitrogen but relatively more sulfur on the surface than for the C1y−NaCl samples. This is probably due to additional undesired sulfur that may have been introduced in the preparation of the DNA solution. We have used DTT in the procedure for MCH cleavage and removal. The residual DTT may result in a higher sulfur concentration on the InAs surface. Therefore, on the basis of the relative measured nitrogen composition, the C1B−NaCl process can be considered the optimum functionalization procedure in the present study. The XPS core spectrum of DNA elements (N and P) and the substrate (In and As) for C1B−NaCl are discussed in Figures 3 and 4.

Table 5. XPS Elemental Compositions for Functionalized Samples

sample	N 1s	P 2p	O 1s	C 1s	S 2p	In 3d	As 3d
C1A−NaCl	5.2	1.9	13.3	45.6	1.9	15.4	16.7
C1B−NaCl	6.2	2.4	15.8	48.3	1.7	13.3	12.4
C1A − no MCH	2.8	1.2	16.3	39.9	4.7	18.4	16.2
C1B − no MCH	2.7	1.9	15.1	41.0	5.5	18.3	15.5

In addition, the sulfur signal is also of interest. The S 2p core-level spectrum consists of $2p_{3/2}$ and $2p_{1/2}$ peaks with an intensity ratio of 2:1 and a spin−orbital splitting of 1.2 eV as shown in Figure 5. Two S 2p components are found at 161.3 and 162.4 eV. The main doublet structure at 162.4 eV is clear evidence of sulfur bound to the substrate as a thiolate, in excellent agreement with previously reported values of thiolates on III−V semiconductors.[24,25,53,54] The minor components at low BE most likely correspond to chemisorbed sulfur on the surface, and the absence of spectral features with BE ≥ 163.5 eV indicates that there are no free thiol groups on the surface.[27,55]

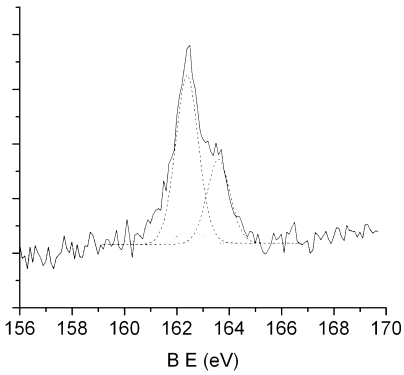

Figure 5. High-resolution XPS spectra of S 2p for C1B−NaCl.

NEXAFS Orientation Studies. The molecular orientation can be determined from the polarization dependence of the NEXAFS intensity. X-ray absorption by molecular orbitals is strongly dependent on the favorable overlap of antibonding orbitals with the electric field (**E**) vector of the incident X-rays.[35] As a result, the polarized X-ray absorption spectra will show differences with the X-ray incident angle for oriented and ordered molecules at surfaces. DNA immobilization is subject to strong mutual electrostatic repulsion rather than van der Waals attraction.[56] Because strands of ssDNA are longer and more flexible than typical molecules used in self-assembled monolayers, long-range lateral ordering is not observed in DNA monolayers.[35,56] The main type of local ordering that may be present in a DNA molecule is nucleobase stacking on average. Figure 6 presents the NEXAFS N K-edge spectra for the C1B−NaCl sample measured at four different incident angles. The spectra contained two major features: a splitting of π^* orbitals in the 399−402 eV region and a broader peak above 405 eV due to the σ^* transition. We assume that the π^* doublet represents an average signal over the four different nucleotide bases. The π^* doublet at lower energy is attributed to nitrogen atoms in the ring structures, and the peak at high energy is consistent with the nitrogen atoms in the nucleobases located next to carbonyl groups. Previous studies on nucleobases[57−60] and DNA oligomers[35,60−62] have shown similar doublet

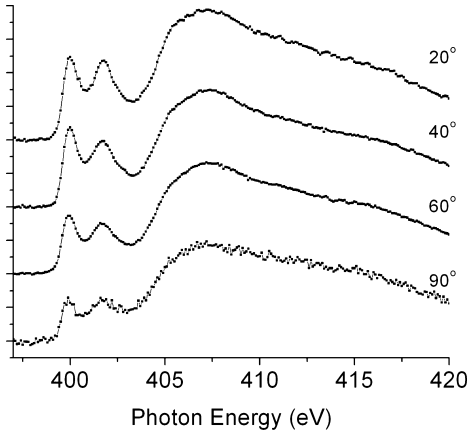

Figure 6. Nitrogen K-edge NEXAFS spectra from mixed DNA/MCH on an InAs surface measured at the angle between normal (90°) and glancing (20°) incident X-ray angles.

dx.doi.org/10.1021/la302313v | *Langmuir* 2012, 28, 11890−11898

features. The π^* resonances are weakest at normal incidence and strongest at grazing incidence, indicating that the DNA bases in the ssDNA were oriented parallel to the surface on average. Because the π^* orbitals lie along the axis of the DNA, the data imply that the axis of the DNA strand tends to project away from the surface.

In the NEXAFS spectra, the intensities of the π^* resonance increase as the angle of the beam relative to the substrate decreases, indicating that the local structure of the DNA molecules possesses a specific orientation on the surface. The angle-dependent transition intensity of the π^* resonance is given by[57]

$$I(\theta) = A\left\{\frac{P}{3}\left[1 + \frac{1}{2}(3\cos^2\theta - 1)(3\cos^2\alpha - 1)\right] + \frac{(1-P)}{2}\sin^2\alpha\right\} \quad (1)$$

where P is the degree of linear polarization of the X-rays, A is the constant describing the angle-integrated cross section, θ is the angle of the beam relative to the substrate plane, and α is the polar angle between the surface normal and the vector of the π^* molecular orbital. Because the employed X-ray beamline was more than 90% linearly polarized, we assumed $P \approx 1$ to ignore the last term in eq 1 for a simpler calculation. Equation 1 can be simplified as[62]

$$I(\theta) = a + b\cos^2\theta \quad (2)$$

yielding values of $a = 0.512 \pm 0.051$ and $b = 0.525 \pm 0.095$. Plots of the peak intensity versus polarization angle for the lower-energy component of the π^* peak are shown in Figure 7.

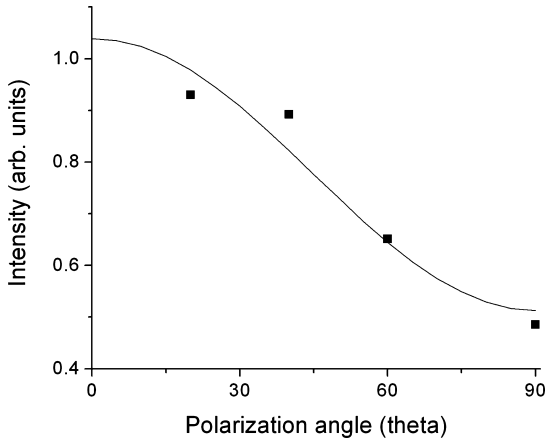

Figure 7. Polarization dependence of the intensities of the π^* resonance in the N K-edge NEXAFS spectra of the C1B−NaCl sample.

A value of α is determined by comparing the coefficients of eqs1 and 2, suggesting an average tilt of the DNA axis of ~45 ± 2° away from the normal combined with a random azimuthal orientation. It is worth noting that the underlying distribution of orientations usually cannot be determined, only an average. This result is consistent with earlier NEXAFS studies of DNA absorbed on the Au surface[56] and on glass and silicon substrates.[62]

CONCLUSIONS

The chemical characterization of the DNA-immobilized InAs surfaces was carried out through XPS and NEXAFS measurements. Before DNA functionalization, the effect of HF- and NH_4OH-based etches on surface oxide removal and prefunctionalization surface chemistry was determined. The DNA functionalization was compared using two methods: method A used a DNA solution containing ammonium hydroxide, and method B used a TE-based DNA solution. Both methods were also used with a 1 M NaCl-based DNA solution. NaCl-based solutions strongly increased the density of immobilized DNA. The presence of DNA was confirmed by F 1s, N 1s, P 2p high-resolution XPS spectra and the P-to-N atomic ratio. The interfacial chemistry of the functionalized surfaces revealed that the thiolated ssDNA probes were immobilized preferentially via In−S bonding with a small fraction of As−S bonding. When both MCH and HS−ssDNA were present in the functionalization solutions, the surface chemistry was modified by the preferential MCH absorption onto As atoms. The C1B−NaCl procedure was found to be the most effective functionalization method, leading to the highest concentration of adsorbed ssDNA. The polarization dependence of NEXAFS N K-edge spectra was used to determine the orbital orientation. The π^* orbitals of nucleobases with a random azimuthal orientation has an average tilt of 45° away from the substrate normal.

ASSOCIATED CONTENT

Supporting Information

Carbon K-edge NEXAFS spectra from mixed DNA/MCH on an InAs surface at normal (90°) and glancing (20°) incident X-ray angles. This material is available free of charge via the Internet at http://pubs.acs.org.

AUTHOR INFORMATION

Corresponding Author

*E-mail: kuech@engr.wisc.edu.

Notes

The authors declare no competing financial interest.

ACKNOWLEDGMENTS

We thank Wenyuan Jiao for assistance with XPS measurements and Phillip Johnson for useful discussions regarding NEXAFS analysis. The NEXAFS experiments were performed at the Synchrotron Radiation Center, University of Wisconsin—Madison. This work was supported by funding from the Defense Advanced Research Projects Agency (DARPA-N66001-09-C-2082).

REFERENCES

(1) Wang, J. *Nucleic Acids Res.* **2000**, *28*, 3011−3016.
(2) Nelson, B. P.; Grimsrud, T. E.; Liles, M. R.; Goodman, R. M.; Corn, R. M. *Anal. Chem.* **2001**, *73*, 1−7.
(3) Tarlov, M. J.; Steel, A. B. In *Biomolecular Films: Design, Function, and Applications*; Rushling, J. F., Ed.; Marcel Dekker: New York, 2003.
(4) Petrovykh, D. Y.; Kimura-Suda, H.; Whitman, L. J.; Tarlov, M. J. J. *Am. Chem. Soc.* **2003**, *125*, 5219−26.
(5) Frutos, A. G.; Liu, Q.; Thiel, A. J.; Sanner, A. M. W.; Condon, A. E.; Smith, L. M.; Corn, R. M. *Nucleic Acids Res.* **1997**, *25*, 4748−4757.
(6) Pang, D.-W.; Zhang, M.; Wang, Z.-L.; Qi, Y.-P.; Cheng, J.-K.; Liu, Z.-Y. *J. Electroanal. Chem.* **1996**, *403*, 183−188.
(7) Hashimoto, K.; Ito, K.; Ishimori, Y. *Anal. Chem.* **1994**, *66*, 3830−3.

(8) Yang, M.; Kong, R. Y. C.; Kazmi, N.; Leung, A. K. C. *Chem. Lett.* **1998**, 257−258.
(9) Souteyrand, E.; Cloarec, J. P.; Martin, J. R.; Wilson, C.; Lawrence, I.; Mikkelsen, S.; Lawrence, M. F. *J. Phys. Chem. B* **1997**, *101*, 2980−2985.
(10) Lamture, J. B.; Beattie, K. L.; Burke, B. E.; Eggers, M. D.; Ehrlich, D. J.; Fowler, R.; Hollis, M. a; Kosicki, B. B.; Reich, R. K.; Smith, S. R. *Nucleic Acids Res.* **1994**, *22*, 2121−2125.
(11) Vo-Dinh, T.; Alarie, J. P.; Isola, N.; Landis, D.; Wintenberg, A. L.; Ericson, M. N. *Anal. Chem.* **1999**, *71*, 358−363.
(12) Strother, T.; Hamers, R. J.; Smith, L. M. *Nucleic Acids Res.* **2000**, *28*, 3535−3541.
(13) Seker, F.; Meeker, K.; Kuech, T. F.; Ellis, A. B. *Chem. Rev.* **2000**, *100*, 2505−2536.
(14) Petrovykh, D. Y.; Yang, M. J.; Whitman, L. *J. Surf. Sci.* **2003**, *523*, 231−240.
(15) Flores-Perez, R.; Zemlyanov, D. Y.; Ivanisevic, A. *ChemPhysChem* **2008**, *9*, 1528−1530.
(16) Mohaddes-Ardabili, L. *J. Appl. Phys.* **2004**, *95*, 6021.
(17) Tsui, D. *Phys. Rev. Lett.* **1970**, *24*, 303−306.
(18) Bhargava, S.; Blank, H.-R.; Narayanamurti, V.; Kroemer, H. *Appl. Phys. Lett.* **1997**, *70*, 759.
(19) Piper, L.; Veal, T.; Lowe, M. *Phys. Rev. B* **2006**, *73*, 195321.
(20) Håkansson, M.; Johansson, L.; Andersson, C.; Karlsson, U.; Olsson, L. Ö.; Kanski, J.; Ilver, L.; Nilsson, P. *Surf. Sci.* **1997**, *374*, 73−79.
(21) Lowe, M.; Veal, T.; McConville, C.; Bell, G.; Tsukamoto, S.; Koguchi, N. *Surf. Sci.* **2003**, *523*, 179−188.
(22) Watanabe, Y.; Maeda, F. *Appl. Surf. Sci.* **1997**, *117*, 735−738.
(23) Giovanelli, L.; Papageorgiou, N.; Terzian, G.; Layet, J. M.; Mossoyan, J. C.; Mossoyan-Deneux, M.; Göthelid, M.; Le Lay, G. *J. Electron Spectrosc.* **2001**, *114−116*, 375−381.
(24) Petrovykh, D. Y.; Smith, J. C.; Clark, T. D.; Stine, R.; Baker, L. A.; Whitman, L. J. *Langmuir* **2009**, *25*, 12185−94.
(25) Tanzer, T. A. T.; Bohn, P. W.; Roshchin, I. V.; Greene, L. H.; Klem, J. F. *Appl. Phys. Lett.* **1999**, *75*, 2794.
(26) Petrovykh, D. Y.; Sullivan, J. M.; Whitman, L. *J. Surf. Interface Anal.* **2005**, *37*, 989−997.
(27) Stine, R.; Petrovykh, D. Y. *J. Electron Spectrosc.* **2009**, *172*, 42−46.
(28) Dedigama, A.; Angelo, M.; Torrione, P.; Kim, T.-H.; Wolter, S.; Lampert, W.; Atewologun, A.; Edirisoorya, M.; Collins, L.; Kuech, T. F.; Losurdo, M.; Bruno, G.; Brown, A. *J. Phys. Chem. C* **2011**, *116*, 826−833.
(29) Fukuda, Y. *Vacuum* **2002**, *67*, 37−41.
(30) Slavin, J. W. J.; Jarori, U.; Zemlyanov, D.; Ivanisevic, A. *J. Electron Spectrosc.* **2009**, *172*, 47−53.
(31) Jewett, S.; Zemlyanov, D.; Ivanisevic, A. *Langmuir* **2011**, *27*, 3774−3782.
(32) Fairley, N. CasaXPS manual: 2.3.15 Spectroscopy; Casa Software Ltd., 2009.
(33) Lau, W.; Sodhi, R.; Jin, S.; Ingrey, S. *J. Vac. Sci. Technol., A* **1990**, *8*, 1899−1906.
(34) Helsen, L.; Van den Bulck, E.; Van Bael, M. K.; Vanhoyland, G.; Mullens, J. *Thermochim. Acta* **2004**, *414*, 145−153.
(35) Lee, C.-Y.; Gong, P.; Harbers, G. M.; Grainger, D. W.; Castner, D. G.; Gamble, L. *J. Anal. Chem.* **2006**, *78*, 3316−3325.
(36) Ptasińska, S.; Stypczyńska, A.; Nixon, T.; Mason, N. J.; Klyachko, D. V.; Sanche, L. *J. Chem. Phys.* **2008**, *129*, 065102.
(37) Herne, T. M.; Tarlov, M. J. *J. Am. Chem. Soc.* **1997**, *119*, 8916−8920.
(38) May, C. J.; Canavan, H. E.; Castner, D. G. *Anal. Chem.* **2004**, *76*, 1114−1122.
(39) Xue, Q. K.; Hashizume, T.; Sakurai, T. *Prog. Surf. Sci.* **1997**, *56*, 1−131.
(40) Voznyy, O.; Dubowski, J. J. *Langmuir* **2008**, *24*, 13299−13305.
(41) McGuiness, C. L.; Shaporenko, A.; Zharnikov, M.; Walker, A. V.; Allara, D. L. *J. Phys. Chem. C* **2007**, *111*, 4226−4234.
(42) Losurdo, M.; Wu, P. C.; Kim, T.-H.; Bruno, G.; Brown, A. S. *Langmuir* **2012**, *28*, 1235−1245.
(43) Cho, E.; Wu, P.; Ahmed, M.; Brown, A.; Kuech, T. F. *Mater. Res. Soc. Symp. Proc.* **2011**, 1301.
(44) Jewett, S.; Zemlyanov, D.; Ivanisevic, A. *J. Phys. Chem. C* **2011**, *115*, 14244−14252.
(45) Knoben, W.; Brongersma, S. H.; Crego-Calama, M. *J. Phys. Chem. C* **2009**, *113*, 18331−18340.
(46) Dannenberger, O.; Weiss, K.; Himmel, H.-J.; Jäger, B.; Buck, M.; Wöll, C. *Thin Solid Films* **1997**, *307*, 183−191.
(47) Zubavichus, Y.; Shaporenko, a.; Grunze, M.; Zharnikov, M. *Nucl. Instrum. Methods Phys. Res., Sect. A* **2009**, *603*, 111−114.
(48) Kaznacheyev, K.; Osanna, A.; Jacobsen, C.; Moruzzi, V. *J. Phys. Chem. A* **2002**, *106*, 3153−3168.
(49) Saenger, W. *Principles of Nucleic Acid Structure*; Springer-Verlag: New York, 1984.
(50) Schroeder, G. K.; Lad, C.; Wyman, P.; Williams, N. H.; Wolfenden, R. P. *Proc. Natl. Acad. Sci. U.S.A.* **2006**, *103*, 4052−4055.
(51) Creager, S. E.; Clarke, J. *Langmuir* **1994**, *10*, 3675−3683.
(52) Kreevoy, M. M.; Harper, E. T.; Duvall, R. E.; Wilgus, H. S., III; Ditsch, L. T. *J. Am. Chem. Soc.* **1960**, *82*, 4899−4902.
(53) McGuiness, C. L.; Shaporenko, A.; Mars, C. K.; Uppili, S.; Zharnikov, M.; Allara, D. L. *J. Am. Chem. Soc.* **2006**, *128*, 5231−5243.
(54) Shaporenko, A.; Adlkofer, K.; Johansson, L. S. O.; Tanaka, M.; Zharnikov, M. *Langmuir* **2003**, *19*, 4992−4998.
(55) Jun, Y.; Zhu, X.-Y.; Hsu, J. W. P. *Langmuir* **2006**, *22*, 3627−3632.
(56) Petrovykh, D. Y.; Pérez-Dieste, V.; Opdahl, A.; Kimura-Suda, H.; Sullivan, J. M.; Tarlov, M. J.; Himpsel, F. J.; Whitman, L. J. *J. Am. Chem. Soc.* **2006**, *128*, 2−3.
(57) Fujii, K.; Akamatsu, K.; Yokoya, A. *J. Phys. Chem. B* **2004**, *108*, 8031−8035.
(58) Furukawa, M.; Fujisawa, H.; Katano, S.; Ogasawara, H.; Kim, Y.; Komeda, T.; Nilsson, A.; Kawai, M. *Surf. Sci.* **2003**, *532−535*, 261−266.
(59) Fujii, K.; Akamatsu, K.; Muramatsu, Y.; Yokoya, A. *Nucl. Instrum. Methods Phys. Res., Sect. B* **2003**, *199*, 249−254.
(60) Kirtley, S. M.; Mullins, O. C.; Chen, J.; van Elp, J.; George, S. J.; Chen, C. T.; O'Halloran, T.; Cramer, S. P. *Biochim. Biophys. Acta* **1992**, *1132*, 249−254.
(61) Vearey-Roberts, A. R. *Appl. Surf. Sci.* **2004**, *234*, 131−137.
(62) Crain, J. N.; Kirakosian, A.; Lin, J.-L.; Gu, Y.; Shah, R. R.; Abbott, N. L.; Himpsel, F. J. *J. Appl. Phys.* **2001**, *90*, 3291.